6-27-2005

Experimental results on the effects of 802.11 b WLAN on networked control system

Chaouki T. Abdallah

Proceedings of the 13th
Mediterranean Conference on Control and Automation
Limassol, Cyprus, June 27-29, 2005

Experimental Results on the Effects of 802.11b WLAN on Networked Control System

R. Sandoval-Rodriguez*, C.T. Abdallah*, H.N. Jerez
Electrical & Computer Engineering Department
MSC01 1100
1 University of New Mexico
Albuquerque, NM 87131-0001
{rsandova,chaouki,hjerez}@ece.unm.edu

R. H. Byrne
Intelligent Systems and Robotics Center
Sandia National Labs
PO Box 5800
Mail Stop 1005
Albuquerque, NM 87185-1005
rhbyrne@sandia.gov

Abstract— **In this paper we expose theoretically and experimentally some of issues induced by wireless Ethernet when it is used to transmit plant state information to the controller, and control signals to the plant, in a closed-loop system. We also propose some compensation actions, and evaluate their performance in the experimental set up.**

I. Introduction

Networked-control applications such as geographically distant sensors gathering information for a remote controller, require state and control signals to travel across communication links. A general purpose communication network will however introduce issues such as propagation time-delays and loss of information. Therefore, the control programs must now account for these issues, and the algorithms should be robust enough to guarantee a certain level of performance. We develop in this paper a series of experiments to identify the issues induced by such a general purpose communication network, with specific emphasis on wireless networks. We use standard operating systems and industrial hardware for data acquisition. Then, we propose compensation alternatives to cope with this issues.

The remainder of the paper is organized as follows, Section II describes the experimental setup implemented to identify these issues and to test the compensation approaches. Section III presents the different issues introduced by 802.11b WLAN. Section IV discusses some approaches to compensate for the issues identified. Section V presents different experiments applying the compensation techniques, and Section VI concludes the papers with a discussion of the results and future research.

II. Experimental Setup

An experimental setup was implemented in order to expose the issues induced by the network. One of the goals is to introduce mobility into the plant, either by physically moving the plant to new locations without the need to rewire the network, or by considering a mobile robot as the plant. A laptop computer is used as the plant's "brain", in order to connect to the building's WLAN using an 802.11b wireless card. A PCMCIA data acquisition card, DAQ 6024E from National Instruments ™, is used to interface the laptop computer to the plant. The software programs used to acquire state data from the sensors, and to apply control signals to the actuators, as well as to implement the communication routines are developed in LabView® also from National Instruments ™. For the controller computer we used various configurations: A laptop computer connected to the building WLAN, a desktop computer connected to the wired building LAN, or a computer with broadband connection outside the campus LAN. The programs in the controller computer, for control and communications, were also developed using LabView®. All computers were running standard Windows XP Professional. Time stamping was used in most of our experiments, and we therefore had to synchronize the computers' clocks. For this purpose, we implemented a routine in LabView®. The controller's computer calculates the time offset, t_{off}, between 'zero marks' in the computers using

$$t_{off} = RTT0 - \left(RTT1 - \left(RTT2 - \frac{RTT3}{2}\right)\right) \quad (1)$$

where the RTT's are as shown Figure 1. The controller's computer then estimates the current time in the plant's computer, t_p, using $t_p = t_c + t_{off}$, where t_c is the current time in the controller's computer. Figure 1 depicts the clock synchronization procedure graphically. The clock's

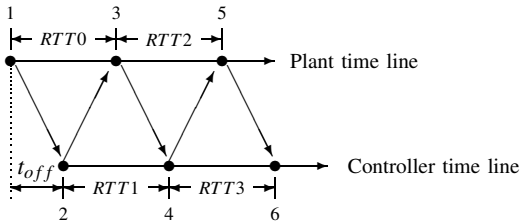

Fig. 1. Clock synchronization procedure.

synchronization routine was implemented using both UDP and TCP over IP. We ran the routine at different times of the

* The research of both authors is partially supported by NSF-0233205 and ANI- 0312611. R. Sandoval-Rodriguez is also with the Chihuahua Institute of Technology.

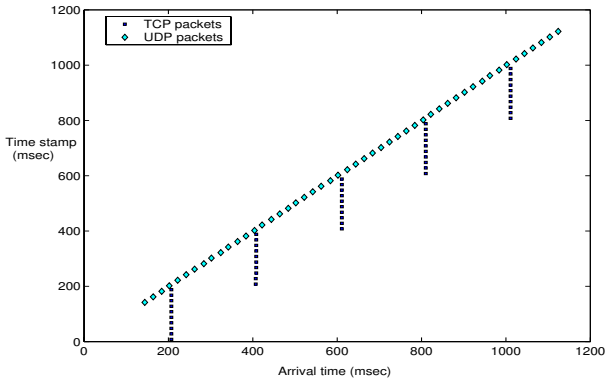

Fig. 2. Arrivals of time stamps using TCP and UDP, sampling at 20msec.

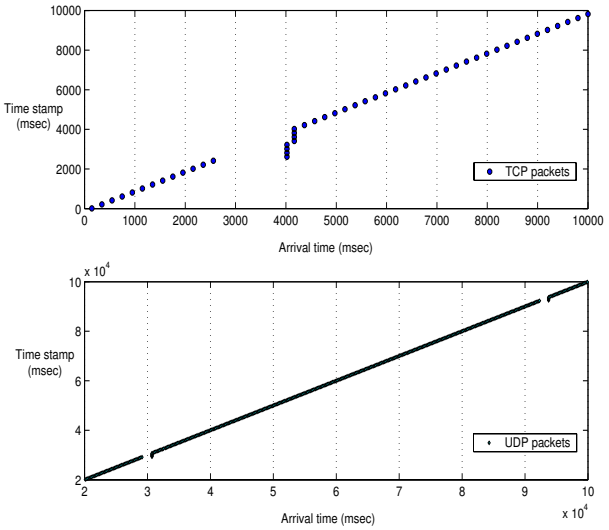

Fig. 3. Disconnection from the WLAN.

day and with the controller's computer inside and outside the building LAN. With the controller's computer inside the building LAN, (whether it is wireless or wired), and during low traffic hours, the average round-trip time was 3msec. During high traffic hours the average round-trip time was 6msec. Having the controller's computer outside the campus LAN, the average round-trip time was 80msec, and no significant difference in the round-trip time was observed at different times of the day. The routine was run before any experiment using time stamping. The estimated error in the clock synchronization is 1msec, which is the resolution in the millisecond timers.

III. Issues introduced by the LAN

A. Retention of Packets

One application in Networked Control Systems is the broadcasting of the plant state's signals to controllers or supervisory monitoring systems. Such broadcasting could be, for instance, the distance to obstacles, or the current heading and speed in a mobile robotic teleoperation. With the purpose of measuring the difference in latency for various sizes of Ethernet packets, we ran a experiment where the plant is transmitting packets with sizes from 46 to 1500 bytes, and alternating between UDP and TCP. With the computer's controller inside the building LAN, we did not observe a significant difference in the latency when transmitting a single packet (independent of its size and using either UDP or TCP). However, when the plant broadcasts packets at a given sampling rate, the 'slow start' feature in TCP limited the broadcasting rate to 200msec, irrespective of the packet size. Even when the signals were sampled at a faster rate, TCP retained the packets until the next multiple of 200msec. Figure 2 shows the arrival time to the controller's computer of time stamps taken at the plant every 20msec; 9 packets were retained and at the next multiple of 200msec, the group of 10 packets were transmitted to the controller's computer. From Figure 2 we see that the samples with time stamps from 20 to 200msec arrived to the controller's computer at $t_c = 200msec$. This problem however, did not manifest itself with UDP packets which arrived every 20msec, as sampled. The retention of packets generates a later bursting of those packets. If the plant's state samples are not time stamped, confusion results at the controller's computer as the program simply can not tell the fresher samples. If bursting occurs, the program in the controller should be able to empty the incoming queue, discard old packets, and only use the last sample of the plant state. We connected the plant's laptop computer to the wired LAN, to verify that this problem occurs with TCP, and not because of the wireless medium. The wired connection did generate the retention of packets when using TCP. Thus, because of the TCP's slow start, if the broadcast requires sampling times smaller than 200msec, our recommendation is to use UDP.

B. Disconnection from the WLAN

Another issue introduced in this case by the wireless network is the disconnection of the plant computer from the WLAN. This problem is attributed to the re-association procedure that the wireless card executes in order to find the access point with the strongest signal. We observed that the disconnection occurs on the average every 60 seconds and lasts on the average, 1.5 seconds. Figure 3 shows the arrival times of time stamps with a disconnection from the WLAN. The top plot shows a disconnection from the WLAN when using TCP and a sampling time of 200msec. The sample with time stamp $t_p = 2410msec$ arrives to the controller at $t_c = 2550msec$, showing a time-delay of $\tau = 140msec$. This time delay includes the delay due to the asynchronism between the retention feature of TCP and the sampling clock in the plant, plus the propagation time-delay. The next sample with time stamp $t_p = 2610msec$ arrives to the controller at $t_c = 4020msec$, showing a time-delay of $\tau = 1410msec$. Subtracting the previous sample time-delay, results in a disconnection time of approximately 1.27sec.

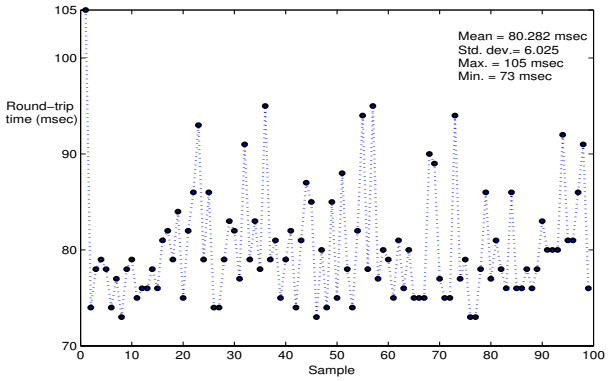

Fig. 4. Round-trip times for 100 samples.

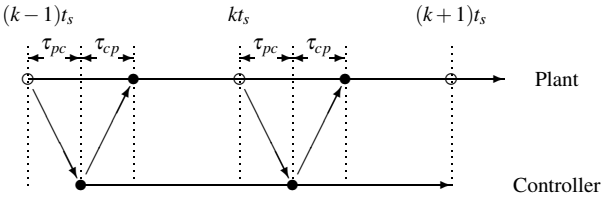

Fig. 5. Time-delay between plant and controller.

The bottom plot in Figure 3 shows the time between two disconnections from the WLAN when using UDP and a sampling time of 200msec. The first disconnection occurred at $t_c = 29133msec$, while the second disconnection occurred at $t_c = 92296msec$, resulting in a time between the disconnections of approximately 63.163sec. The time of disconnection, and the period between disconnections seem to be independent of the congestion control protocol and sampling time used.

C. Propagation Time-Delay

For this experiment the controller's computer was connected to a broadband ISP outside the building's LAN, with the purpose of emphasizing the problem of large time-delays. We again ran the experiment of reading the plant's clock as a time stamp and sending it to the controller's computer, which sends it back immediately. The plant's computer registers the arrival times and computes the round-trip times. Figure 4 shows the resulting round-trip times of 100 samples. In order to check for symmetry in the channel, we calculated the average arrival time at the controller's computer, resulting in 41msec, fairly symmetric with respect to the average RTT of Figure 4 which resulted 80.282msec. We ran these experiments several times at different times of the day. The mean of the round-trip times changed slightly, but the standard deviation was relatively constant. The plant-to-controller and controller-to-plant time-delays were verified to be close, thus establishing that the propagation channel is symmetric. With the purpose of illustrating the effect of time-delay and to set a basis for the compensation schemes to be presented in Section IV, let us consider the scalar system

$$\dot{x} = ax + bu \tag{2}$$

where $a > 0$, and $b > 0$. Let us also consider state (in this case also output) feedback control with gain K, i.e. $u = -Kx$. The sensing is clock-driven with sampling time t_s, and the control and actuation are event-driven. This means that the controller will compute and send a control signal as soon as it receives a sample, and that the plant will immediately process any received control signal. The time-delay between the plant and the controller is denoted by τ_{pc}, while the time-delay between the controller and the plant is denoted by τ_{cp}, as depicted in Figure 5. At this time, we consider that the combined time-delay is less than the sampling time. We observe that the control signal $u = -Kx[(k-1)t_s]$ arrives to the plant at time $(k-1)t_s + \tau_{pc} + \tau_{cp}$, and is held until time $kt_s + \tau_{pc} + \tau_{cp}$, when it is replaced by the new control signal $u = -Kx[kt_s]$. Thus, two control signals are applied during the interval $kt_s \le t \le (k+1)t_s$. Solving for the system's state in equation (2) in the interval $kt_s \le t \le kt_s + \tau_{pc} + \tau_{cp}$, yields

$$x[kt_s + \tau_{pc} + \tau_{cp}] = \Phi_1 x[kt_s] + \Gamma_1 x[(k-1)t_s] \tag{3}$$

where

$$\begin{aligned} \Phi_1 &= e^{a(\tau_{pc}+\tau_{cp})} \\ \Gamma_1 &= -\frac{b}{a}K\left(e^{a(\tau_{pc}+\tau_{cp})} - 1\right) \end{aligned}$$

Now, solving for the interval $kt_s + \tau_{pc} + \tau_{cp} \le t \le (k+1)t_s$, results

$$x[(k+1)t_s] = \Phi_2 x[kt_s + \tau_{pc} + \tau_{cp}] + \Gamma_2 x[kt_s] \tag{4}$$

where

$$\begin{aligned} \Phi_2 &= e^{a(t_s-\tau_{pc}-\tau_{cp})} \\ \Gamma_2 &= -\frac{b}{a}K\left(e^{a(t_s-\tau_{pc}-\tau_{cp})} - 1\right) \end{aligned}$$

Substituting (3) into equation (4), and simplifying

$$x[(k+1)t_s] = \Psi x[kt_s] + \Upsilon x[(k-1)t_s] \tag{5}$$

where

$$\begin{aligned} \Psi &= e^{at_s} - \frac{b}{a}K\left(e^{a(t_s-\tau_{pc}-\tau_{cp})} - 1\right) \\ \Upsilon &= -\frac{b}{a}K\left(e^{at_s} - e^{a(t_s-\tau_{pc}-\tau_{cp})}\right) \end{aligned}$$

Consider now the augmented vector

$$y[kt_s] = \begin{bmatrix} x[kt_s] \\ x[(k-1)t_s] \end{bmatrix} \tag{6}$$

leading to the augmented system

$$y[(k+1)t_s] = \Phi y[kt_s] \tag{7}$$

where

$$\Phi = \begin{bmatrix} \Psi & \Upsilon \\ 1 & 0 \end{bmatrix} \tag{8}$$

Thus, given the system parameters a and b, control gain K, and sampling time t_s, there exists an upper bound, τ^*, in the combined time-delay $\tau = \tau_{pc} + \tau_{cp}$, such that if $\tau < \tau^*$ the matrix Φ in equation (8) is Schur. In other words, the system can tolerate the combined time-delay $\tau = \tau_{pc} + \tau_{cp}$, and still converge to the origin.

IV. Compensation Approaches

The use of time stamping in the plant's samples, along with clock synchronization between the plant and controller computers, allows the controller to estimate the time elapsed in the plant since the last received plant sample was taken. If in addition, the plant sends to the controller the last control signal applied, also time stamped, and assuming knowledge of the plant's model, the controller can estimate the current state of the plant, then generate a more accurate control signal. The following subsections present compensation approaches for the propagation time-delay and the network disconnection, assuming the conditions mentioned above.

A. Compensating for plant-to-controller Time-delay

Assuming that the plant transmits to the controller state samples with time stamp t_{ps}, and the last control signal applied with time stamp t_{cs}, then the plant-to-controller time-delay can be obtained from $\tau_{pc} = t_c + t_{off} - t_{ps}$, where t_c is the sample arrival time at the controller, and t_{off} is the offset time between the plant and controller clocks. For the sake of simplicity, we consider zero computation time for the control signal. Now, using the elapsed time τ_{pc}, the controller can estimate the current state of the plant, and uses that estimate to generate the control signal. Using again Figure 5, the control signal $u = -K\hat{x}[(k-1)t_s + \tau_{pc}]$ arrives at the plant at time $(k-1)t_s + \tau_{pc} + \tau_{cp}$, and is applied and held until the next control signal $u = -K\hat{x}[kt_s + \tau_{pc}]$ arrives to the plant at time $kt_s + \tau_{pc} + \tau_{cp}$. We can solve for the state of the system in equation (2) in the interval $kt_s \le t \le (k+1)t_s$, in the following steps:

$$x[kt_s + \tau_{pc}] = \Phi_3 x[kt_s] + \Gamma_3 x[(k-1)t_s + \tau_{pc}] \quad (9)$$

where

$$\Phi_3 = e^{a\tau_{pc}} \qquad \Gamma_3 = -\frac{b}{a}K(e^{a\tau_{pc}} - 1)$$

$$\begin{aligned} x[kt_s + \tau_{pc} + \tau_{cp}] &= \Phi_4 x[kt_s + \tau_{pc}] \\ &\quad + \Gamma_4 x[(k-1)t_s + \tau_{pc}] \end{aligned} \quad (10)$$

where

$$\Phi_4 = e^{a\tau_{cp}} \qquad \Gamma_4 = -\frac{b}{a}K(e^{a\tau_{cp}} - 1)$$

$$x[(k+1)t_s] = \Phi_5 x[kt_s + \tau_{pc} + \tau_{cp}] + \Gamma_5 x[kt_s + \tau_{pc}] \quad (11)$$

where

$$\Phi_5 = e^{a(t_s - \tau_{pc} - \tau_{cp})} \qquad \Gamma_5 = -\frac{b}{a}K(e^{a(t_s - \tau_{pc} - \tau_{cp})} - 1)$$

$$x[(k+1)t_s + \tau_{pc}] = \Phi_6 x[kt_s + \tau_{pc} + \tau_{cp}] + \Gamma_6 x[kt_s + \tau_{pc}] \quad (12)$$

where

$$\Phi_6 = e^{a(t_s - \tau_{cp})} \qquad \Gamma_6 = -\frac{b}{a}K(e^{a(t_s - \tau_{cp})} - 1)$$

$$\begin{aligned} x[(k+1)t_s + \tau_{pc} + \tau_{cp}] &= \Phi_7 x[kt_s + \tau_{pc} + \tau_{cp}] \\ &\quad + \Gamma_7 x[kt_s + \tau_{pc}] \end{aligned} \quad (13)$$

where

$$\Phi_7 = e^{a(t_s)} \qquad \Gamma_7 = -\frac{b}{a}K(e^{at_s} - 1).$$

Defining now the augmented vector

$$v[kt_s] = \begin{bmatrix} x[kt_s + \tau_{pc} + \tau_{cp}] \\ x[kt_s + \tau_{pc}] \\ x[kt_s] \\ x[(k-1)t_s + \tau_{pc} + \tau_{cp}] \\ x[(k-1)t_s + \tau_{pc}] \end{bmatrix} \quad (14)$$

the augmented system becomes

$$v[(k+1)t_s] = \Phi_{pc} v[kt_s] \quad (15)$$

where

$$\Phi_{pc} = \begin{bmatrix} \Phi_7 & \Gamma_7 & 0 & 0 & 0 \\ \Phi_6 & \Gamma_6 & 0 & 0 & 0 \\ \Phi_5 & \Gamma_5 & 0 & 0 & 0 \\ 0 & \Phi_4 & 0 & 0 & \Gamma_4 \\ 0 & 0 & \Phi_3 & 0 & \Gamma_3 \end{bmatrix} \quad (16)$$

For the purpose of illustration, let us consider the following example.

Example 1: Let the system's parameters be $a = 1$, $b = 1$, $K = 2$, the sampling time $t_s = 500msec$, and the propagation time-delays, $\tau_{pc} = 100msec$ and $\tau_{cp} = 100msec$. Substituting these parameters in the transition matrix of equation (8), for the original uncompensated system, its eigenvalues are found to be $(0.4745 \pm 0.6104i)$, which lie inside the unit circle. Now let us increase the propagation time-delays to $\tau_{pc} = \tau_{cp} = 250msec$, which correspond to one sample delay control. Substituting again the parameters in equation (8), the eigenvalues are found to be $(0.8244 \pm 0.7860i)$. Note that the eigenvalues now lie outside the unit circle. Using compensation for the propagation time-delay τ_{pc}, we find the eigenvalues in equation (16) to be $(0, -0.5681, 0, 0.5403 \pm 0.6614i)$. All the eigenvalues now lie inside the unit circle, and in spite of the large propagation time-delays, the compensation scheme makes the system converge to the origin.

B. Compensating for controller-to-plant Time-delay

In the previous subsection, the estimate of the plant state, $\hat{x}[kt_s + \tau_{pc}]$, was computed based on the measured time-delay τ_{pc}. The resulting control signal $u = -Kx[kt_s + \tau_{pc}]$ generated will arrive at the plant with a time-delay τ_{cp}, but unfortunately, at the time of computing the control signal, this controller-to-plant time-delay is unknown. However, assuming that we have the time stamps of the previous control signals applied to the plant, we can obtain an estimate of the next controller-to-plant time-delay. So, considering

that this prediction of τ_{cp} is accurate with some degree of confidence, we can estimate the plant's state at the time of arrival of the control signal. Proceeding in a similar fashion to the previous subsection, the state of the system in equation (2), in the interval $kt_s \leq t \leq (k+1)t_s$, can be obtained in the following steps:

$$\begin{aligned} x[kt_s+\tau_{pc}] &= \Phi_3 x[kt_s] \\ &\quad +\Gamma_3 x[(k-1)t_s+\tau_{pc}+\tau_{cp}] \end{aligned} \tag{17}$$

$$\begin{aligned} x[kt_s+\tau_{pc}+\tau_{cp}] &= \Phi_4 x[kt_s+\tau pc] \\ &\quad +\Gamma_4 x[(k-1)t_s+\tau_{pc}+\tau_{cp}] \end{aligned} \tag{18}$$

$$\begin{aligned} x[(k+1)t_s] &= \Phi_5 x[kt_s+\tau_{pc}+\tau_{cp}] \\ &\quad +\Gamma_5 x[kt_s+\tau_{pc}+\tau_{cp}] \end{aligned} \tag{19}$$

$$\begin{aligned} x[(k+1)t_s+\tau_{pc}] &= \Phi_6 x[kt_s+\tau_{pc}+\tau_{cp}] \\ &\quad +\Gamma_6 x[kt_s+\tau_{pc}+\tau_{cp}] \end{aligned} \tag{20}$$

$$\begin{aligned} x[(k+1)t_s+\tau_{pc}+\tau_{cp}] &= \Phi_7 x[kt_s+\tau_{pc}+\tau_{cp}] \\ &\quad +\Gamma_7 x[kt_s+\tau_{pc}+\tau_{cp}] \end{aligned} \tag{21}$$

The parameters Φ_3 to Φ_7, and Γ_3 to Γ_7, are the same as in the previous subsection. Considering again the augmented vector of equation (14), the augmented system compensating for both time-delays is given by:

$$v[(k+1)t_s] = \Phi_\tau v[kt_s] \tag{22}$$

where

$$\Phi_\tau = \begin{bmatrix} \Phi_7+\Gamma_7 & 0 & 0 & 0 & 0 \\ \Phi_6+\Gamma_6 & 0 & 0 & 0 & 0 \\ \Phi_5+\Gamma_5 & 0 & 0 & 0 & 0 \\ 0 & \Phi_4 & 0 & \Gamma_4 & 0 \\ 0 & 0 & \Phi_3 & \Gamma_3 & 0 \end{bmatrix} \tag{23}$$

Again, for illustration purposes, let us use the following example.

Example 2: Let us consider the same system parameters as in example 1, but assume now the time sampling is $t_s = 700msec$ and the propagation time-delays $\tau_{pc} = \tau_{cp} = 300msec$. Substituting the parameters in the transition matrices of equations (8) and (16), we obtain the eigenvalues $(0.9017 \pm 1.0020i)$ and $(0, -0.6997, 0, 0.5151 \pm 0.8824i)$ respectively. Even with the compensation for the plant-to-controller time-delay, the complex conjugate eigenvalues lie outside the unit circle. Applying compensation for both time-delays, we substitute the parameters in the transition matrix of equation (23), with the eigenvalues resulting $(0, -0.6997, 0, 0, -0.0138)$. All the eigenvalues lie inside the unit circle. Despite the large propagation time-delays, the compensation scheme for both time-delays makes the system converge to the origin.

C. Compensating for Disconnection from the WLAN

Now, consider the case of disconnection from the network, or equivalently of dropped packets. The effects of this issue on the networked-closed-loop system will depend on the stability of open-loop plant, and on the state of the plant at the time of the disconnection. In the case of an open-loop stable plant, a sufficiently large disconnection will move the plant towards an equilibrium point defined by the control signal being applied at the time of disconnection. However, in an open-loop unstable plant, the plant states will continue to increase exponentially in the direction they were moving at the time of disconnection. Fast dynamics plants may get out of control, but for some slower dynamics plants, this might be a recoverable situation. In [5], we gave upper bounds on the time that an unattended unstable system can stay inside its region of attraction, assuming saturation in the control signal. We can use those results to decide if the plant should hold the last control signal applied, or if it should apply zero control signal when a disconnection is detected. Considering the system in equation (2), and assuming the saturation values $\pm u_{max}$ in the control signal, there exists a region of attraction (see [5]) defined by the interval $-x_{max} = -\frac{b}{a}u_{max} < x < \frac{b}{a}u_{max} = x_{max}$. In order to find the best control action that the plant should apply in case of a disconnection, whether to hold the last control signal $u(t_d)$ or to apply zero control signal, we can use the expression of the state for system (2) and solve for the time t_e, at which the plant state leaves the region of attraction $\pm x_{max}$, given an initial condition $x(t_d)$. Considering first the case of applying zero control signal, the time t_e at which the plant state, with initial condition $x(t_d) > 0$, will reach the positive edge, x_{max}, of the region of attraction is given by

$$t_e = \frac{1}{a}\ln\left(\frac{x_{max}}{x(t_d)}\right) \tag{24}$$

Now, considering that the plant holds the last control signal applied $u(t_d) = -Kx(t_d)$, and assuming state feedback with initial condition $x(t_d) > 0$, the time t_e at which the plant state reaches the negative edge, $-x_{max}$ is given by

$$t_e = \frac{1}{a}\ln\left(\frac{-x_{max} - \frac{aK}{b}x(t_d)}{x(t_d) - \frac{aK}{b}x(t_d)}\right) \tag{25}$$

Rearranging terms

$$t_e = \frac{1}{a}\ln\left(\frac{x_{max}}{x(t_d)(\frac{aK}{b}-1)} + \frac{\frac{aK}{b}}{\frac{aK}{b}-1}\right) \tag{26}$$

For values of $\frac{aK}{b}$ in the interval $2 > \frac{aK}{b} > 1$, the time t_e in equation (26) for which the system can be unattended is larger than the one in equation (24). In this case holding the last control signal will give the system a better chance to recover from the disconnection.

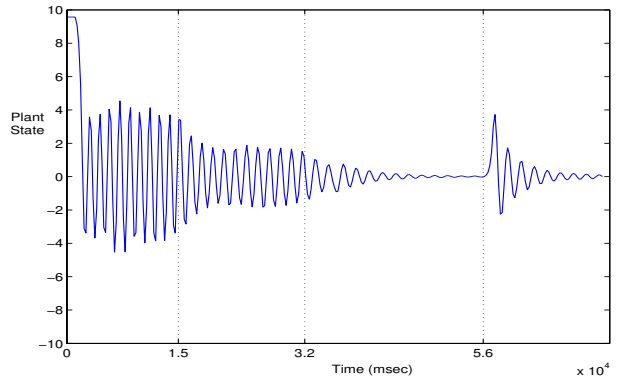

Fig. 6. Response of the plant states with time-delay, and compensations later applied.

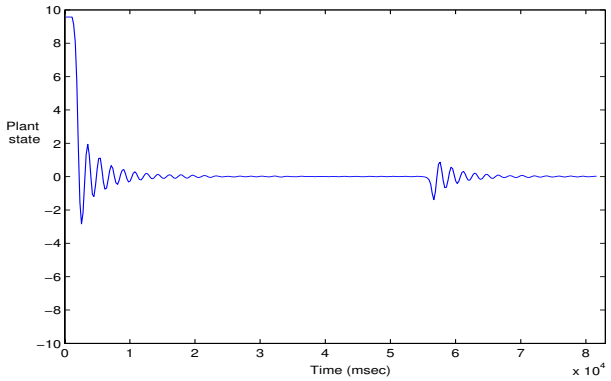

Fig. 7. Response of the plant states to time-delay, and compensations applied.

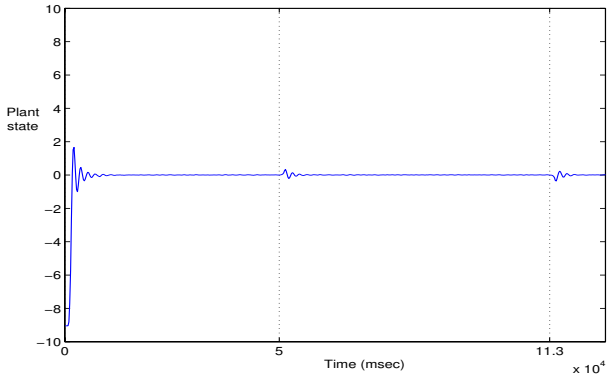

Fig. 8. Response of the plant states to time-delay, and compensations applied.

V. Experimental results

In order to evaluate the performance of the time-delay compensation approaches, and considering the disconnection cases as proposed in Section IV, we implemented the system in equation (2) as an electronic circuit having the approximate model $\dot{x} = 3.2x + 3.2u$, this circuit is then considered as our physical plant. We used as the controller a computer connected outside the campus LAN, and applied state feedback with gain $K = 2$. The round-trip time was on the average around 80msec, as shown in Figure 4, and the one-way trips were fairly symmetric. In the first experiment we used a sampling time $t_s = 240msec$. Figure 6 shows the response to the initial condition $x(0) = 9.6$ volts. For the first 15sec no compensation was applied and the plant state oscillates between ± 4 volts. At $t = 15sec$ compensation for the plant-to-controller time-delay τ_{pc} is applied, which reduces the oscillations to ± 2 volts. At $t = 32sec$ compensation for the controller-to-plant time-delay τ_{cp} is also applied, and this reduces the oscillations almost to zero. At $t = 56sec$ a disconnection occurs, but the system is able to recover from it. In the second experiment we used a sampling time $t_s = 220msec$, but in this case the compensations for both time-delays were applied since $t = 0$. Figure 7 shows the response to the initial condition $x(0) = 9.6$ volts. We can see that despite the time-delay, the system converges to zero after 25 seconds. At time $t = 55sec$ a disconnection occurs and the system is able to recover from it with less oscillations than in the first experiment.

In the third experiment we used a sampling time $t_s = 200msec$, and the compensations for both time-delays were also applied at $t = 0$. Figure 8 shows the response to the initial condition $x(0) = -9.6$ volts. Two disconnections occurred, the first at $t = 50sec$, and the second at $t = 113sec$, but the system suffered a minimum level of disruption.

VI. Conclusions and future work

We have identified in this paper issues induced by a wireless network, which as far as we know had not been reported before. We also presented compensation algorithms for propagation time-delay and evaluated these approaches in an experimental set-up with satisfactory results. Future work will include the analysis of these issues combined with saturation and quantization effects, the limited network bandwidth, and the generation of robust algorithms that work under such constraints for scalar and multivariate systems.

References

[1] L. A. Montestruque, P. J. Antsaklis, "Model-Based Networked Control Systems-Stability", ISIS Technical Report ISIS-2002-001, Department of Electrical Engineering, University of Notre Dame, January 2001.

[2] G. C. Walsh, Y. Hong, L. G. Bushnell, "Stability Analysis of Networked Control Systems", IEEE Transactions on Control Systems Technology, Vol. 10, No. 3, pp. 438-446, May 2002.

[3] D. Mills, "Internet time synchronization: The network time protocol", IEEE Transactions on Communications, vol. 39, pp. 1482-1493, Oct. 1991.

[4] N. J. Ploplys, P. A. Kawka, A. G. Alleyne,"Closed-Loop Control over Wireless Networks, Developing a novel timing scheme for real-time control systems", IEEE Control Systems Magazine, June 2004.

[5] R. Sandoval R., C. T. Abdallah, R. H. Byrne, "Effects of Quantization, Saturation, and Sampling Time in Multi Output Systems", 43^{rd} IEEE Conference on Decision and Control, Atlantis, Paradise Island, The Bahamas, December 2004.

[6] W. Zhang, M. S. Branicky, S. M. Phillips, "Stability of Networked Control Systems", IEEE Control Systems Magazine, February 2001, pp. 84-99.